Thermochimica Acta, 231 (1994) 307-315
Elsevier Science B.V., Amsterdam
SSDI 0040-6031(93)01356-8

Thermal oxidation of indium nitride films

Yutaka Sawada * and Akira Hashimoto [1]

Department of Industrial Chemistry, Faculty of Engineering, Tokyo Institute of Polytechnics, 1583 Iiyama, Atsugi-shi, Kanagawa 243-02 (Japan)

(Received 31 March 1993; accepted 10 May 1993)

Abstract

Thermal oxidation of sputter-deposited indium nitride films has been investigated in air at the heating rate of 10°C min^{-1}. Surface oxidation occurred at 300–350°C and many domes were formed. Complete formation of In_2O_3 occurred with a drastic increase in the resistivity at 400–500°C when the domes were destroyed. Formation and destruction of the domes is explained by the volume increase from the nitride to the oxide. The oxidized films are sensitive to water vapour and ammonia.

INTRODUCTION

Indium nitride, a III–V semiconductor with wide direct band gap has been studied for potential applications in the visible light optoelectric devices and low-cost solar cells with high efficiency [1–9]. Takai [10] reported a multicolored electrochromism of indium nitride films. Surface oxidation of indium nitride films at room temperature was reported by Foley and Lyngdal [6]. Natrajan et al. [11] and Eltoukhy et al. [12] attempted the deposition of oxynitride films by a sputtering method under an atmosphere of nitrogen–oxygen mixture.

Thermodynamically, the oxidation reaction ($2InN + (3/2)O_2 = In_2O_3 + N_2$) was expected to occur under almost any available experimental conditions [13–16]. However, to the best of our knowledge, the mechanism of oxidation has not been clarified completely. In the present study, the thermal oxidation of indium nitride films has been investigated.

EXPERIMENTAL

Nitride films

Indium nitride films were deposited by r.f. (13.56 MHz) magnetron sputtering (Anelva SPF-210H) using a metallic target (purity 99.999%, diameter 100 mm, thickness 5 mm). The system was evacuated to a

* Corresponding author.
[1] Present address: Dipsol. Co. Ltd., 3-8-10 Shinkoiwa Katsushika-ku, Tokyo 124, Japan.

0040-6031/94/$07.00 © 1994 – Elsevier Science B.V. All rights reserved

background pressure of 1×10^{-6} Torr (nitrogen equivalent) with an oil-diffusion pump ($300\,l\,s^{-1}$) and a liquid-nitrogen trap. Corning 7059 glass substrates (25 mm × 75 mm × 0.4 mm) were cleaned ultrasonically and boiled in trichloroethylene. The substrate was r.f. sputter-etched (100 W, 2 min) with argon (purity 99.999%, pressure 3×10^{-3} Torr). The indium nitride films were deposited by the reactive sputtering method onto the water-cooled substrate in nitrogen atmosphere (purity 99.9995%, pressure 2×10^{-3} Torr, mass flow rate 1 std.$cm^3\,min^{-1}$). The target–substrate distance was 7 cm and the deposition rate was 34 nm min^{-1}. The target power was restricted to 50 W since the indium target melted when higher power was applied. Transparent films were obtained in the first several batches; this could be attributed to an oxide layer on the surface of the metallic target. Reproducible nitride formation was achieved after 10 batches (approximately 5 h of total deposition time).

Dependence of the peak-to-peak signals of the Auger electron spectra on the ion-etching time for the surface of the as-deposited film is shown in Fig. 1. Detection of nitrogen suggests nitride formation. The detection of nitrogen at the surface suggests that the nitride is not completely covered with the surface oxide layer; the escape depth of the Auger electron is about 1 nm. Oxygen should be attributed to the coexistence of the oxide or formation of oxynitride proposed by Natrajan et al. [11], Eltoukhy et al. [12] and Westra and Brett [9]. Carbon should be attributed to the surface contaminant adsorbed from the atmosphere. The films were reddish-brown (dark red). The optical spectra for the as-deposited films are shown in Fig. 2. The band gap was 1.83–1.91 eV which was within the range of the reported values; 1.9 eV [2], 1.89–2.18 eV [5], 1.70 eV [9] and 1.7–2.4 eV [11]. The X-ray diffraction of the film did not give any peak but only a halo, while Foley and Tansley [17] detected peaks for their films. The film surface observed by SEM (magnification 10 000, not shown) was flat and smooth.

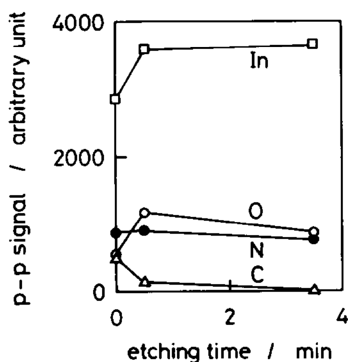

Fig. 1. Dependence of the peak-to-peak signals of the Auger electron spectra on the ion-etching time for the as-deposited film: etching gas, argon; acceleration voltage of the ion, 1 kV; etching rate (estimated), 1 nm min^{-1}.

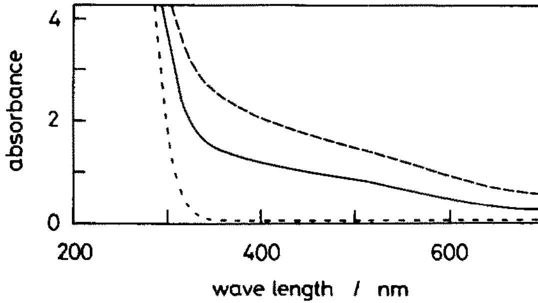

Fig. 2. Optical spectra for the as-deposited films of thickness 170 nm (—) and 102 nm (– – – –), and for the substrate without the film (----).

The volume resistivity ($(1.06–1.32)\times10^{-3}\,\Omega\,cm$) was approximately independent of the film thickness and was lower than the reported values; $3\times10^{-3}\,\Omega\,cm$ [9, 10], $4\times10^{-2}\,\Omega\,cm$ [18] and $1\times10^{-1}\,\Omega\,cm$ [19].

Thermal oxidation and characterization

The specimens were heated in air and oxygen (1 atm) at the heating rate of $10°C\,min^{-1}$. Electrical resistance during the heating was monitored by the four-point-probe method; four stripes of electrodes were constructed with a silver paste on the surface of the film.

The specimens were analyzed with a scanning Auger microscope (Jeol JAMP-30 and JAMP-7100). To minimize film damage by the electron beam, the acceleration voltage and the beam current were lowered for most of the analysis: 5 kV and 2.6×10^{-8} A, respectively. The films were reduced to metallic indium when ion-etched with argon (acceleration voltage 3 kV). In most of the present analyses, the films were ion-etched at the lower acceleration voltage (1 kV). However, the possibility of ion damage could not be completely neglected considering the report by Foley and Lyngdal [6].

The surface roughness for the specimen was measured with a SEM (Elionics EMM-300) with a couple of secondary electron detectors whose signals were transformed into the surface roughness. X-Ray diffraction was measured with a conventional (θ–2θ type) diffractometer with nickel filtered copper radiation (40 kV, 25 mA). The optical absorption was measured with a conventional spectrometer (Hitachi U-3200). The film thickness at the as-deposited condition was measured by optical interference (Anelva Nanoscope).

RESULTS

Thermal change in resistivity

The electrical resistance of the films during heating in air are shown in Fig. 3. The same results were obtained upon heating in an oxygen flow. The

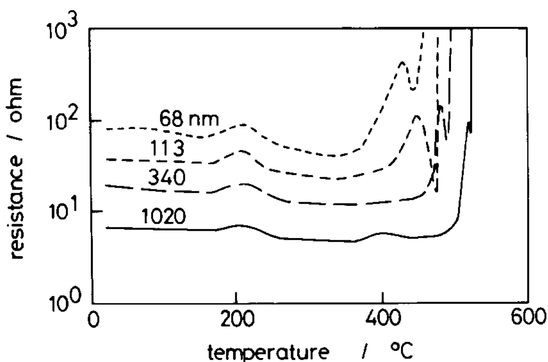

Fig. 3. Resistance of films during heating in air at a heating rate of 10°C min^{-1}. Film thickness is indicated in the figure.

partial pressure of oxygen (0.2 and 1.0 atm) did not affect the oxidation reaction under the present experimental conditions. A small peak at about 200°C was not elucidated completely but it is probably due to the thermal change of the silver paste, since a change in the texture was observed at the silver electrodes. The resistance was approximately constant until 350°C; the constant resistivity suggests that the nitride film remained unchanged. The temperature coefficient (slightly negative) of the resistivity until about 350°C can be explained by the semiconductive behavior of the nitride. A drastic increase in the resistivity at 430–520°C should be attributed to oxidation. A small peak observed prior to the drastic increase was not clarified in the present study. These changes (the small peak and the drastic increase in resistivity) occurred at lower temperatures for the thinner films; this suggests that the rate of oxidation was affected by the film thickness.

When the film (thickness about 100 nm) was quenched at approximately 400°C, i.e. immediately after the increase in the resistivity was observed, the resistivity continued to increase. The color changed from reddish brown to transparent; movement of the color boundary was clearly observed. The self-inductive nature of the reaction can be explained by an exothermic reaction for the oxidation [13–16].

Quenched films

200°C

No difference was found for the films quenched from 200°C during the heating (heating rate 10°C min^{-1}); the color, surface morphology and X-ray diffraction remained unchanged from those of the unheated ones.

300°C

The scanning electron micrographs for the films quenched from 300°C are shown in Fig. 4. Many domes were observed. The height of a typical dome is shown in Fig. 5. The heights were about 10–15% of the radius on

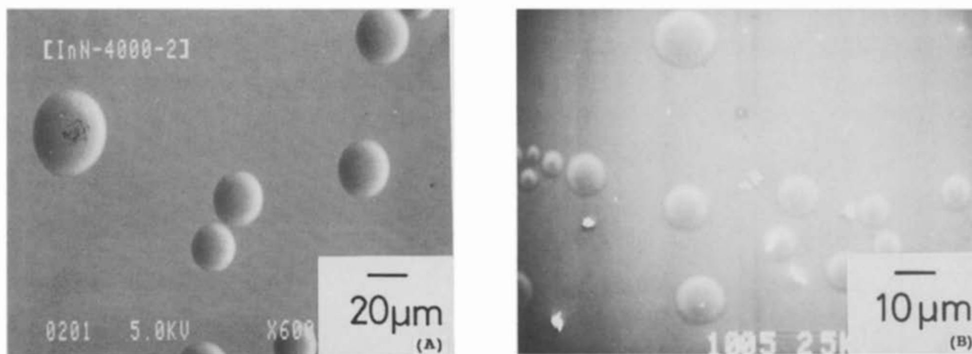

Fig. 4. Scanning electron micrographs for the film quenched from 300°C, film thickness, 340 nm. (A) the film was tilted, and (B) the film was normal to the primary electron beam of the SEM, respectively.

the skirt of the dome for all the specimens in the present study. The relation between the dome radius and the film thickness is shown in Fig. 6. The dome radius was approximately proportional to the film thickness. The film thickness corresponded to about 2% of the radius of curvature. The dependence of the peak-to-peak signals of the Auger electron spectra on the ion-etching time for the films is shown in Fig. 7. The oxidation of the film was indicated by the disappearance of nitrogen and the increase of the O/In ratio compared with Fig. 1. No detection of carbon could be attributed to the nature of the fully oxidized surface on which less carbon contaminant adsorbs. The compositional difference between the top of the dome and the flat portion of the film was negligible.

No marked changes were observed in color, resistance or X-ray diffraction. These results suggest that the major portion, i.e. the inner portion of the films, remained unchanged from the as-deposited conditions.

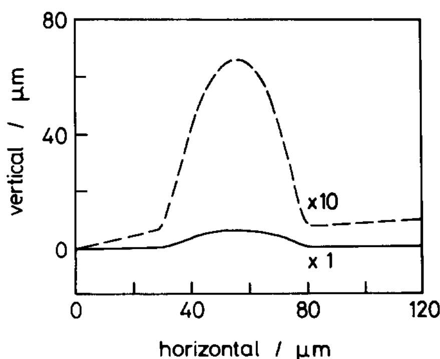

Fig. 5. Height of a typical dome for the films quenched from 300°C; film thickness, 1020 nm.

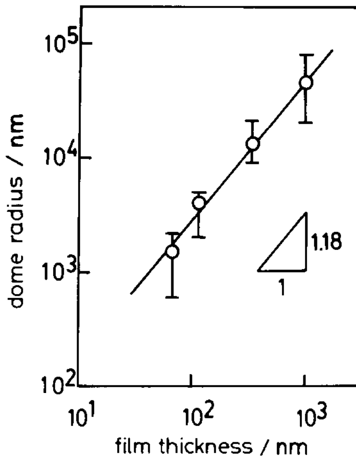

Fig. 6. Relation between dome radius and film thickness for films quenched from 300°C. The radius was measured at the skirt of the dome.

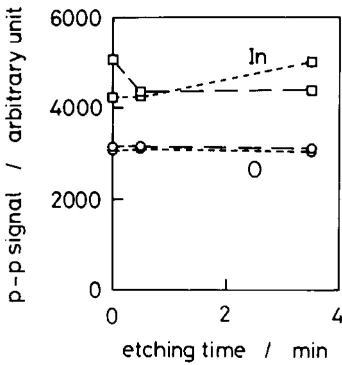

Fig. 7. Dependence of the peak-to-peak signals of the Auger electron spectra on the ion-etching time for the film quenched from 300°C. Top of the dome (————), flat portion of the film (----). Analytical conditions were the same as those of Fig. 1.

500°C

The micrographs for the films quenched from 500°C are shown in Fig. 8. Many domes were cracked along the skirt so that the substrate was

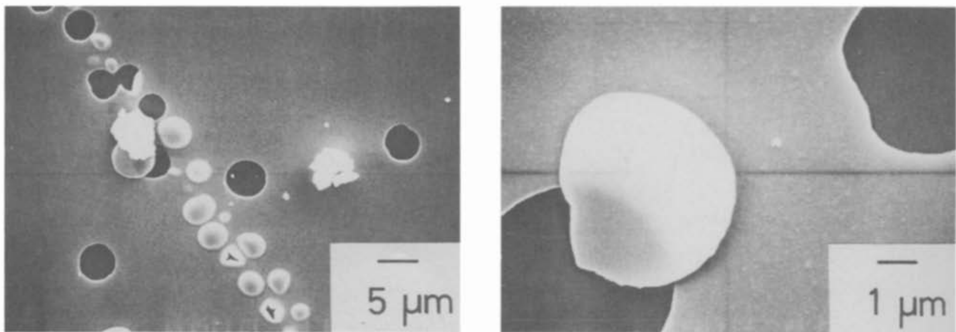

Fig. 8. Scanning electron micrographs for the films quenched from 500°C; film thickness, 113 nm. The vertical and horizontal lines are the traces of the electron beam for the measurement of the surface roughness.

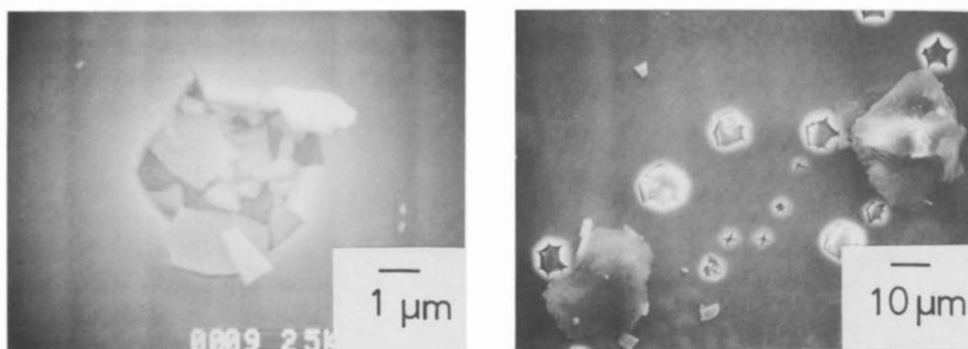

Fig. 9. Scanning electron micrographs for the thicker films quenched from 500°C; film thickness, 340 nm.

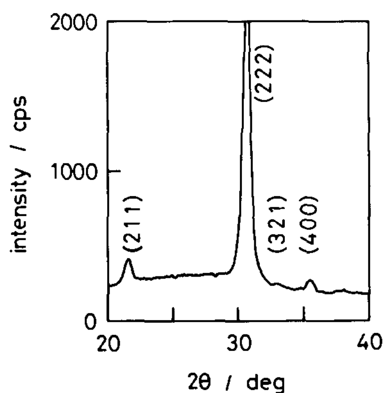

Fig. 10. X-Ray diffraction pattern for the films quenched from 500°C; film thickness, 340 nm.

exposed. Destruction of the domes for the thicker films occurred at the top as shown in Fig. 9; a dome fractured into many pieces. The films were transparent (colorless). The X-ray diffraction pattern is shown in Fig. 10. The interplanar distances agreed with that of In_2O_3 [20]; (222) preferred orientation was observed. These results suggests that the film was oxidized completely.

DISCUSSION

The morphological change of the films during heating is schematically illustrated in Fig. 11. The dome formation in Fig. 11(2) should be attributed to the stress induced by the surface oxidation of the nitride film; the volume increase from the nitride to the oxide (approximately 4.6%) estimated from the bulk data [20, 21] supports this hypothesis. Similar domes were observed [22] after thermal oxidation (500°C, 1 h in air) of tungsten oxide films (thickness, 300 nm) which was sputter-deposited onto a heated or unheated glass substrate in argon atmosphere using a WO_3 target. Dome formation seems to occur at the portion where the adhesion between the

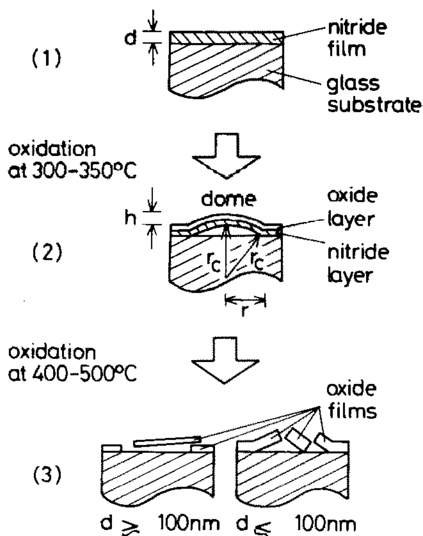

Fig. 11. Schematic illustration of the morphological change during the heating in air of indium nitride films: d, film thickness measured for the as-deposited condition; h, height of the dome; and r_c radius of curvature.

film and the substrate is relatively weak. The insufficient adhesion may be caused by contaminants or defects on the substrate surface, etc. This hypothesis seems to be supported by Fig. 8 (right hand photo) where the domes are systematically disposed. The destruction of the domes in Fig. 11(3) was explained by the reverse transformation (from the dome to the flat pieces) by the oxidation at the inner portion of the film. Flatness of the broken pieces in Figs. 8 and 9 supports this hypothesis.

The resistance of the fully oxidized films fluctuated remarkably at room temperature. The resistance slightly decreased when water vapor (breath) or ammonia gas (from ammonia water) was intentionally blown onto the film. The resistance recovered when the film was blown with hot air from a hair drier. The gas sensitive nature can be explained by microcracks or micropores in the flat portion of the oxidized films, although the resolution of the SEM was insufficient to detect them.

ACKNOWLEDGMENT

The authors thank Mr. Y. Nagasawa (Jeol Ltd.) for scanning Auger analysis.

REFERENCES

1 J.B. MacChesney, P.M. Bridenbaugh and P.B. O'Connor, Mater. Res. Bull., 5 (1970) 783.
2 H.J. Hovel and J.J. Cuomo, Appl. Phys. Lett., 20 (1972) 71.

3 K. Osamura, S. Naka and Y. Murakami, J. Appl. Phys., 46 (1975) 3432.
4 T.L. Tansley and C.P. Foley, Electron. Lett., 20 (1984) 1066.
5 T.L. Tansley and C.P. Foley, J. Appl. Phys., 59 (1986) 3241.
6 C.P. Foley and J. Lyngdal, J. Vac. Sci. Technol. A, 5 (1987) 1708.
7 B.T. Sullivan, R.R. Parsons, K.L. Westra and M.J. Brett, J. Appl. Phys., 64 (1988) 4144.
8 A. Wakahara and A. Yoshida, Appl. Phys. Lett., 54 (1989) 709.
9 K.L. Westra and M.J. Brett, Thin Solid Films, 192 (1990) 227.
10 O. Takai, Kinzoku Hyomen Gijyutsu, 35 (1984) 71.
11 B.R. Natarajan, A.H. Eltoukhy, J.E. Greene and T.L. Barr, Thin Solid Films, 69 (1980) 217.
12 A.H. Eltoukhy, B.R. Natarajan, J.E. Greene and T.L. Barr, Thin Solid Films, 69 (1980) 229.
13 I. Barin and O. Knacke, Thermochemical Properties of Inorganic Substances, Springer Verlag, Berlin, 1973 p. 495.
14 I. Barin and O. Knacke, Thermochemical Properties of Inorganic Substances, Springer Verlag, Berlin, 1973, p. 584.
15 I. Barin, O. Knacke and O. Kubaschewski, Thermochemical Properties of Inorganic Substances, Suppl., Springer Verlag, Berlin, 1977, p. 318.
16 I. Barin, O. Knacke and O. Kubaschewski, Thermochemical Properties of Inorganic Substances, Suppl., Springer Verlag, Berlin, 1977, p. 327.
17 C.P. Foley and T.L. Tansley, Appl. Surf. Sci., 22 (1985) 663.
18 B.R. Natarajan, A.H. Eltoukhy, J.E. Greene and T.L. Barr, Thin Solid Films, 69 (1980) 201.
19 T.J. Kistenmacher and W.A. Bryden, Appl. Phys. Lett., 59 (1991) 1844.
20 Joint Committee for Powder Diffraction File, 6-416 (1955).
21 Joint Committee for Powder Diffraction File, 2-1450 (1938)
22 Y. Sawada, unpublished.